



Influence of aging temperature on phase transformation and mechanical behavior of NiTi thin films deposited by magnetron sputtering technique

Hamed Daneshvar¹, Mir Saman Safavi¹, Vida Khalili², Jafar Khalil-Allafi^{*1}

¹Research Center for Advanced Materials, Faculty of Materials Engineering, Sahand University of Technology, Tabriz, Iran.

²Department of Materials Science and Engineering, University of Bonab, Bonab, Iran.

Received: 14 May 2020; Accepted: 3 June 2020

* Corresponding author email: allaifi@sut.ac.ir

ABSTRACT

In this study, NiTi thin films were deposited on the glass and NaCl substrates by means of magnetron sputtering method. The influence of aging temperature, over the range 300–500 °C, on phase transformation and mechanical properties of the sputtered NiTi thin films were studied by differential scanning calorimetry (DSC) and nano-indentation assay, respectively. The DSC curves showed that the aged specimens at 350, 400, and 500 °C underwent two steps transformation during cooling process while a three steps transformation has been observed for the film aged at 450 °C. This behavior clearly demonstrated the heterogeneity in chemical composition and microstructure of the sputtered thin film, which consequently resulted in the martensitic transformation of R and remained B2 to B19' within two steps. According to nano-indentation analysis results, a peak point at aging temperature of 450 °C is reached. The temperature hysteresis of all aged films was about 1 °C, which can be considered as a positive sign for sensor application.

Keywords: NiTi thin film, Magnetron sputtering, Aging temperature, Mechanical behavior, Phase transformation, sensor.

1. Introduction

NiTi thin films have been widely used for fabrication of micro actuator, sensors, and micro electromechanical systems (MEMS) owing to their acceptable sensitivity to the temperature and stress variations [1]. As the surface-to-volume ratio of NiTi thin film is higher than that of bulk state, a quick cooling as well as rapid response to the environmental changes can be achieved by thin films [2, 3]. Large displacement, great damping capacity, high actuation force, and low operating voltage are the other features of NiTi thin films that made them as a suitable candidate to be broadly used in MEMS [4].

In order to obtain a superior shape memory

effect in NiTi thin film, it is wise to control the chemical composition, particularly equiatomic ratio of Ni:Ti [5]. NiTi alloys show two steps phase transformation from (i) ordered cubic (B2) to the trigonal (R)-phase. (ii) In the second step B2 and R phase transforms to the monoclinic phase (M) B19'. The B19' phase is occasionally referred to as martensite. It is well known that only a 1 at.% Ni change in NiTi chemical composition can vary transformation temperature of Ni-rich NiTi thin film by 100 °C [6]. Till date, a broad variety of empirical techniques such as flash evaporation [7], pulsed laser deposition [8], filtered arc deposition [9], co-electrodeposition [10], electron beam evaporation [11], and magnetron sputtering [12],

[13] have been utilized to prepare NiTi thin films. The magnetron sputtering carried out at ambient temperature is a well-developed route to produce NiTi thin film. However, it is not possible to state that the sputtered coating has the similar composition to that of target. There are some operational factors including sputtering yield, angular distribution, and sticking coefficient that may vary the amount of deposited Ni and Ti during the sputtering process [14]. The sputtering yield has the biggest impact on abovementioned inequality, and can be defined as the fraction of the detached atoms from the surface of target to the collided atoms on the surface of substrate. The higher sputtering yield of Ni results in generation of a film with higher Ni concentration than that of target. On the other hand, the higher tendency of Ti to form Ti oxides may noticeably decrease its concentration in the structure of sputtered film [15]. Described below three potential approaches to prepare NiTi thin film with desired composition during magnetron sputtering method: (i) using a Ti-rich NiTi target [16], (ii) co-sputtering from two separate Ni and Ti targets [17], and (iii) co-sputtering from two separate Ti and NiTi targets [18]. It can be easily expect that a significant difference in overall characteristics of these films may be generated when various approaches was employed for thin film fabrication. For instance, Tillmann et al. [14] have reported the feasibility of sputtering from single Ti-rich NiTi target. It should be mentioned that a favorable mechanical and tribological properties can be achieved through the deposition of layered composite thin films [19]. However, the satisfactory use of these thin films still faces several challenges such as insufficient tribomechanical properties. The major drawback of NiTi thin film deposited by magnetron sputtering at ambient temperature is formation of an amorphous structure without shape memory effect and superelastic behavior [20]. Such a film should be crystallized by either appropriate in-situ annealing process or post-annealing [4]. The aging process has been widely employed to vary the overall properties of NiTi shape memory alloy through phase transformations. However, whether the applied aging process can alter the transformation behavior of the NiTi greatly depends on its temperature. The aim behind the application of the aging treatment in the temperature range of 350-550 °C is to improve the shape memory effect and superelasticity as well as controlling the phase transformation temperatures. On the

other hand, the application of aging treatment at room temperature lead to the formation of nano-precipitates [21-24]. The in-situ annealed thin film may demonstrate higher adhesion to the substrate together with lower residual stress compared to post-annealed one [20]. It is to be noted that a poor bonding strength and high residual stress can be considered as an advantage, especially when the aim is to detach the thin film from the substrate. Deposition of a buffer layer between the substrate and top layer is other proposed way to detach the deposited thin film [25]. The importance of easy detachment from substrate is highlighted when the sputtered films are supposed to undergo post heat treatment. The detached NiTi films provide a substrate for production of miniaturized Nitinol devices which can be extensively used in medical and other industrial applications [26].

The aim of this research is to investigate the effects of aging temperature on phase transformation and mechanical properties of NiTi thin films deposited by magnetron sputtering using Ti-rich NiTi single target.

2. Materials and methods

NiTi thin films were deposited using Ti-rich NiTi single target (Ti-46.7 at.%Ni) via a high voltage magnetron sputtering apparatus (Mega2000™, France). The prepared target was re-melted three times in the vacuum chamber followed by annealing at 900 °C for 24 h to increase its microstructural homogeneity. The as-cast Ti-rich NiTi alloy was machined to a have diameter of 76 mm and a thickness of 6.6 mm. The deposition time was 6 h. Table 1 outlines the operating conditions applied for deposition of NiTi thin film.

The NaCl substrate was used to facilitate the sputtered films detachment, i.e., obtaining freestanding films for DSC analysis. Similarly, the glass substrate played same role to prepare favorable samples for SEM and nanoindentation studies.

The cross-sectional morphology and chemical composition of the sputtered thin films was evaluated using scanning electron microscopy

Table 1- The operating conditions applied for deposition of NiTi thin film. Base

Base pressure	2.3×10^{-6} mbar
Deposition rate	1.8 Å s ⁻¹
Power	370 W
Voltage	400 V
Substrate	Glass & NaCl

(SEM, Cam Scan MV2200, Vega TescanTM, Czech Republic) coupled with energy dispersive spectroscopy (EDS, Oxford Instrument Mod 7378), respectively.

The microstructural properties of the sputtered films was characterized by X-ray diffractometer (XRD, Advance-D8, BrukerTM, Germany) using CuK α radiation source, in the 2θ range from 20 to 60° at a step size of 0.02° with scan rate of 1.8 (2θ sec⁻¹).

The detached films from NaCl substrates were post annealed at 550°C for 1 hour and aged at different temperatures, namely 350, 400, 450, and 500°C for 90 min in a quartz tubes contained Ti getters, which were isolated under a vacuum of 1×10^{-5} mbar to prevent the oxidation of thin films.

Differential scanning calorimetry (DSC, 404 C calorimeter, NetzschTM, Germany) was used to determine the temperatures of phase transformations. DSC measurements were carried out at heating/cooling rate of 10 °C min⁻¹ from -100°C to 150°C for the annealed specimens.

The hardness and elastic modulus of the aged thin films were assessed using nanoindentation technique (Nano Indenter XP MTS TM, USA). The nanoindentation analysis was performed in a controlled constant maximum penetration depth of 210 nm by a Berkovich indenter. The typical loading-penetration depth curves were recorded during the loading time of 30 s, holding time of 10 s, and unloading time of 30 s. The hardness and elastic modulus of the thin films were extracted by an approach presented by Oliver-Pharr [27].

Generally, the loading-penetration depth curves consist two regions, as follows: (i) the area under the unloading curve which correlates to the amount of reversible elastic work (W_e) and (ii) closed area of

the curve that corresponds to the plastic work (W_p). The total mechanical work (W_t) is calculated using the following Equation (1):

$$W_t = W_e + W_p \quad (1)$$

3. Results and discussion

3. 1. Morphological and microstructural assays

The EDS analysis results of as-sputtered NiTi thin film are presented in Fig. 1.

Results show the formation of a film with 50.31 at.% Ni and 49.69 at.% Ti, which meets the required range for inducing shape memory effect, in accordance with the literature [19]. The cross-section SEM image of NiTi thin film sputtered on glass substrate is depicted in Fig. 2.

As can be seen, a 4 μ m thick film is formed on the substrate. As the substrate is being kept at ambient temperature during sputtering procedure, the atoms reached to the substrate may cool down with an extremely high cooling rate, and consequently there is not enough time for the reaching atoms to deposit in an ordered sequence. The high kinetic energy of the sputtered atoms should also be taken into considerations. This is why an amorphous structure is generated [28]. Fig. 3 illustrates the XRD patterns of the as-sputtered and post-annealed NiTi thin films at 550°C for 1 hour followed by water quench.

A broad peak appeared in Fig. 3-a demonstrates that the sputtered NiTi film has a characteristics of amorphous structure. From Fig. 3-b, sharper peaks emerged at $2\theta=43.46^\circ$ and 63.16° with (110) and (200) crystallographic planes of austenite B2 phase in NiTi, respectively. These results obtained in accordance with the reference code of 00-019-0850 in PDF2 database. The main B2 peak shifts

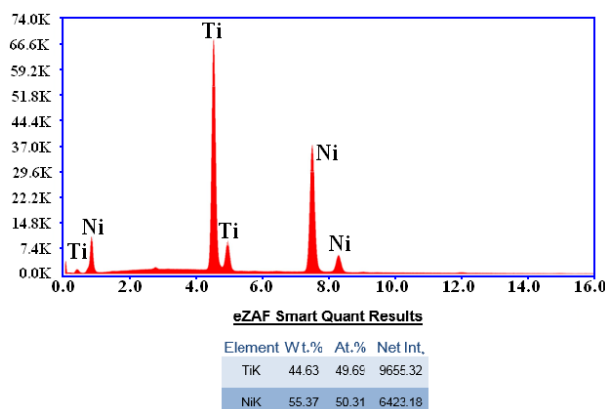


Fig. 1- The EDS analysis results of as-deposited NiTi thin film.

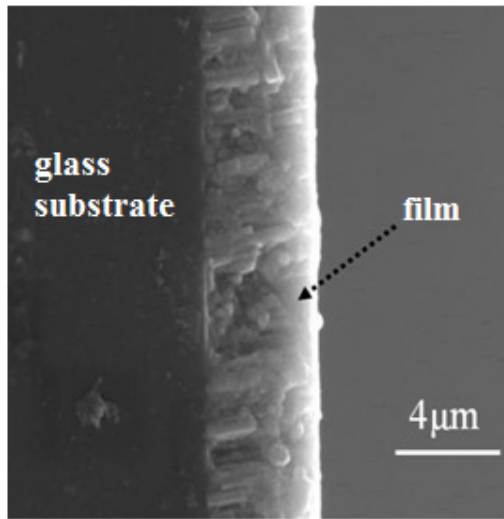


Fig. 2- The cross-section SEM image of the as-deposited NiTi thin film on the glass substrate.

toward more positive values due to the generated residual stresses during the process. Moreover, the peaks corresponded to the martensitic B19' phase in NiTi at $2\theta=34.8^\circ$ and 41.3° are identified according to the reference code of 00-035-1281. Also, the reflected peak at $2\theta=46.4^\circ$ is assigned to (202) crystallographic plane of Ni_3Ti phase that is identified based on the reference code of 01-075-0878.

3. 2. Phase transformations

DSC analysis was performed in the temperature range of -10 to 150°C to evaluate the effects of aging temperature on martensitic transformation behavior. The DSC curves recorded at various aging temperatures are shown in Fig. 4.

The reflected peaks for all studied films in Fig. 4 show the thermoelastic and reversible transformations from Martensite to Austenite phase during heating and cooling, which are responsible for inducing the shape memory effect. The phase transformation temperatures impress materials response to deformation [13]. From Fig. 4, the first peak in the DSC curves of studied films is attributed to B2→R phase transformation, which appears at the almost same temperature of 104°C during cooling. It implies that aging at various temperatures did not change the B2→R phase transformation temperature. A peak emerged at DSC curves of aged samples, except that aged at 450°C, is related to the transformation of R→B19' and

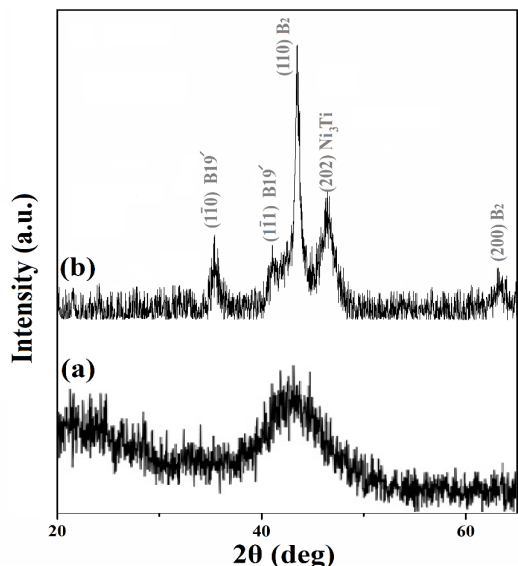


Fig. 3- The XRD patterns of the (a) as-sputtered NiTi film and (b) NiTi films post-annealed at 550°C for 1 hour followed by water quench.

remained B2→B19'. The R phase can be formed in the vicinity of Ni-rich precipitates such as Ni_4Ti_3 and Ni_3Ti due to their stress fields [24, 29-32]. The presence of aforementioned precipitates in the microstructure of aged films at 350 °C and 450 °C is demonstrated in Fig. 5. It is to be noted that the XRD test has been carried out at the temperature that was shown by vertical arrows in Fig. 4-a and Fig. 4-c.

In the mentioned temperatures, there is a mixture of B2 and B19' phases in the structure of aged films. Notably, the nucleation barrier for R phase (~1 % shear stress) is lower than that of B19' phase (~10 % shear stress). Therefore, during cooling the high temperature B2 phase transforms to monoclinic martensitic B19' via trigonal intermediate R phase [30]. It is to be noted that there are both Ni-rich and Ti-rich precipitates in the microstructure of aged NiTi thin films, thus it can be concluded that a heterogeneity in chemical composition is generated. Turning again to Fig. 4-c, the curve composed of three peaks during cooling. The peaks denoted as (2) and (3) are related to R→B19' and B2→B19' transformations, respectively. Thus, it can be inferred that the martensitic transformation in this sample occur in three steps which majorly arise from a high precipitation rate. Similarly, Khalil-Allafi et al. [24, 31, 32] have reported the high precipitation rate of Ni_4Ti_3 particles during aging process. These particles composed of 57.1 at.% Ni which surrounded by Ti-rich zones. Ni

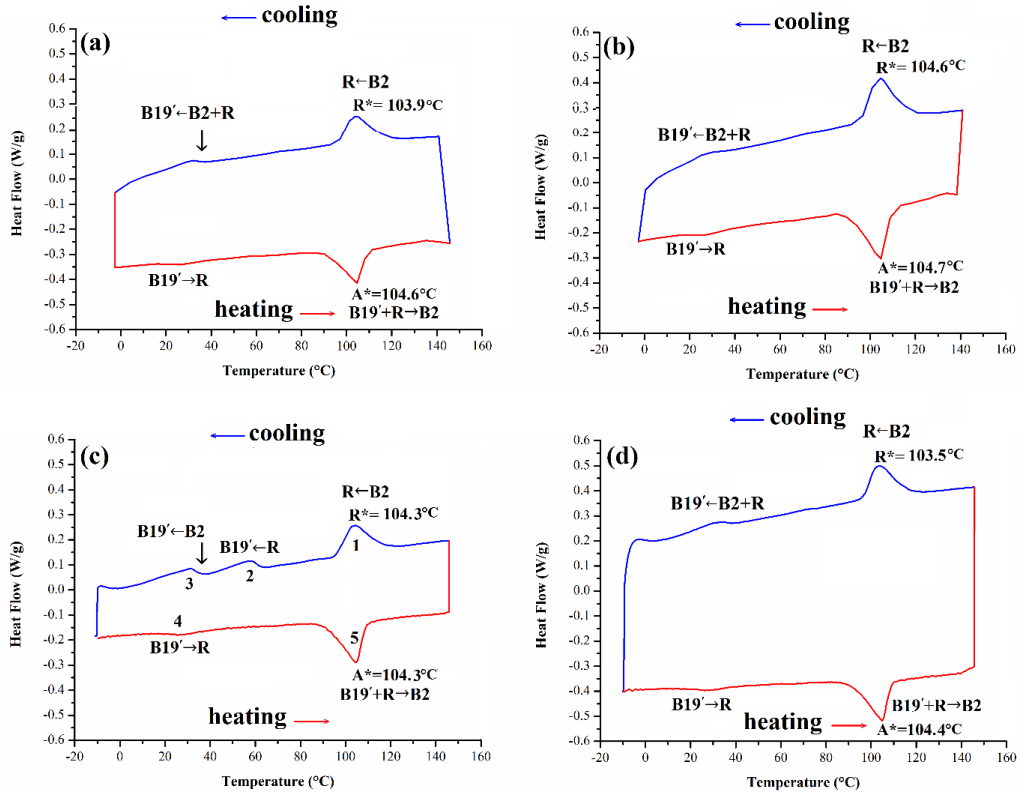


Fig. 4- DSC curves recorded at various aging temperatures: (a) 350 °C, (b) 400 °C, (c) 450 °C, and (d) 500 °C.

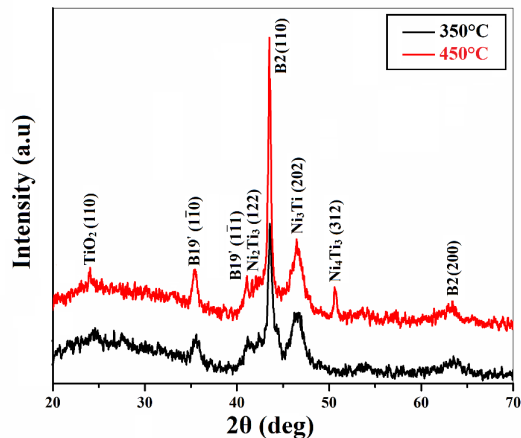


Fig. 5- The XRD spectra of the aged NiTi films at 350 and 450°C for 90 min followed by water quenching.

depletion around these precipitates leads to a shift of martensitic transformation temperatures towards higher values. In addition, peaks (2) and (3) in Fig. 4-c can be attributed to the martensitic phase transformation in the vicinity and farther areas of precipitates, respectively. To sum up, both R and B19' phases appear in the vicinity of

Ni_4Ti_3 precipitates as a result of coherent stress fields. Indeed, the first peak during cooling is related to B2→R phase transformation, while the second one is corresponded to R→B19' phase transformation in the presence of coherent stress fields around the Ni_4Ti_3 . Third peak on cooling is ascribed to B2→B19' phase transformation within

coherent stress-free fields. There can be seen two peaks in the heating regime irrespective of aging temperature. A two steps phase transformation, i.e. $B19' \rightarrow R$ and $B19' + R \rightarrow B2$ is also observable in the heating regime.

Meanwhile, a detailed description of theories that dealt with multiple-step martensitic transformation in the bulk NiTi has been presented elsewhere [24, 29-32]. According to the results, there is an almost same $B2 \rightarrow R$ phase transformation temperatures with approximately $1^{\circ}C$ difference, during heating (A^*) and cooling (R^*) cycles in all of studied cases. Therefore, the temperature hysteresis of all aged films was about $1^{\circ}C$, which can be considered as a positive sign for sensor application.

For micro-actuator applications, the martensitic phase of NiTi film should be stable at room temperature [33]. The results of DSC analysis of aged NiTi films meet this requirement.

3. 3. Mechanical behavior

Fig. 6 depicts the typical load-indentation depth curves of aged NiTi thin films as a function of aging temperature.

A small plateau at constant load of P_{max} in the presented curves is due to the holding time of 10

s at this point. Also, the continuity in the loading curves without any pop-in ascribed to the absence of phase transformation such as stress induced martensite since the measurements were performed at room temperature, i.e. lower temperature than M_f in cooling regime. The calculated elastic modulus (E) and hardness (H) values of the aged NiTi films at different temperatures are compared in Fig. 7.

Both H and E enhance with increase in aging temperature up to $450^{\circ}C$ followed by a decrease with further temperature rise to $500^{\circ}C$. The rate of nucleation and growth of precipitation is the predominant factor governing the mechanical behavior of the aged NiTi films, wherein a slow growth rate of precipitations is observed for films aged at $350^{\circ}C$ and $400^{\circ}C$. On the other hand, the growth rate of precipitation at $500^{\circ}C$ is higher than that aged at $450^{\circ}C$, while the nucleation rate at aging temperature of $450^{\circ}C$ is higher than that of $500^{\circ}C$. This may lead to the formation of fine precipitates with uniform distribution throughout the microstructure of the film that aged at $450^{\circ}C$ followed by increasing the precipitation hardening and critical stress of dislocation slip, which results in E and H increment [31].

There is a direct relationship between P_{max}

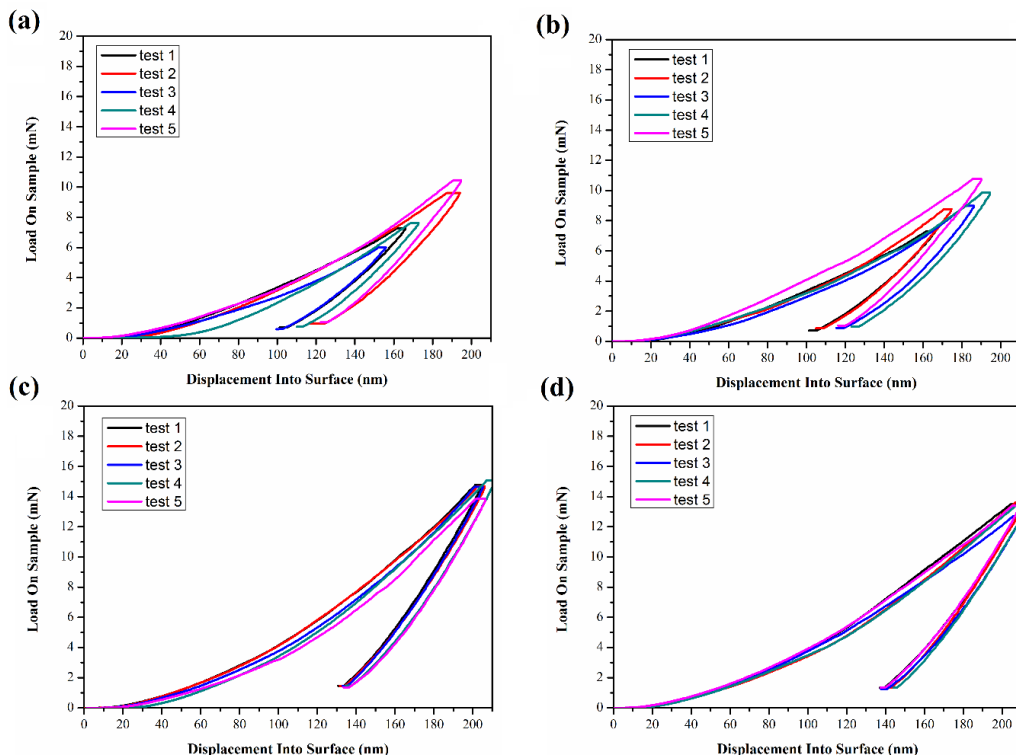


Fig. 6- The typical load-indentation depth curves of NiTi thin films aged at: (a) $350^{\circ}C$, (b) $400^{\circ}C$, (c) $450^{\circ}C$, and (d) $500^{\circ}C$.

and hardness values in Oliver-Pharr equation [34]. The maximum H (22.52 ± 1.13 GPa) and P_{\max} (14.61 ± 0.46 mN) values obtained for the film aged at 450°C . P_{\max} values of NiTi films aged at 350, 400, and 500°C are 8.20 ± 1.81 , 9.13 ± 1.30 , and 13.34 ± 0.37 mN, respectively. The presence of the uniformly distributed small precipitates with high stiffness over the structure of film that aged at 450°C significantly contributes to its strengthening. The reason why E and H values in this work are higher than those reported by Behera et al. [35] is related to the formation of dense structure.

Fig. 8 indicates the extracted values of W_p and W_e from the load-indentation depth curves versus aging temperature. W_p is more than W_e irrespective of aging temperature. The aged NiTi film at 450°C possesses the highest W_p and W_e . More W_p is required to penetrate into the controlled depth of 210 nm in the case of hard film. Moreover, according to Fig.7 and

Fig. 8, a high elastic modulus induces more reversible W_e .

4. Conclusions

In this study, NiTi thin films were successfully deposited on the glass and NaCl substrates using magnetron sputtering technique by means of Ti-rich NiTi single target. The influences of post aging temperature on phase transformation behavior and mechanical properties of the as-sputtered thin films are reported. The aged films at 350, 400, and 500°C consisted two steps phase transformation, while the film aged at 450°C showed three steps phase transformation during cooling cycle. The temperature hysteresis of all aged films was about 1°C , which can be considered as a positive sign for sensor application. The nanoindentation studies revealed that aging the as-sputtered NiTi films at 450°C significantly improves the elastic modulus and hardness values.

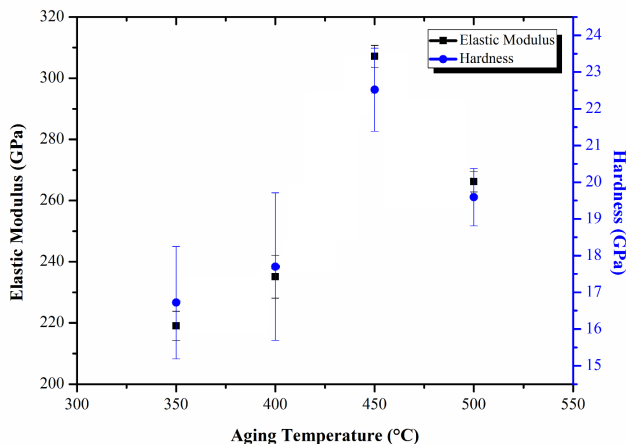


Fig. 7- The elastic modulus and hardness values of NiTi films aged in the temperature range of $350\text{-}500^{\circ}\text{C}$.

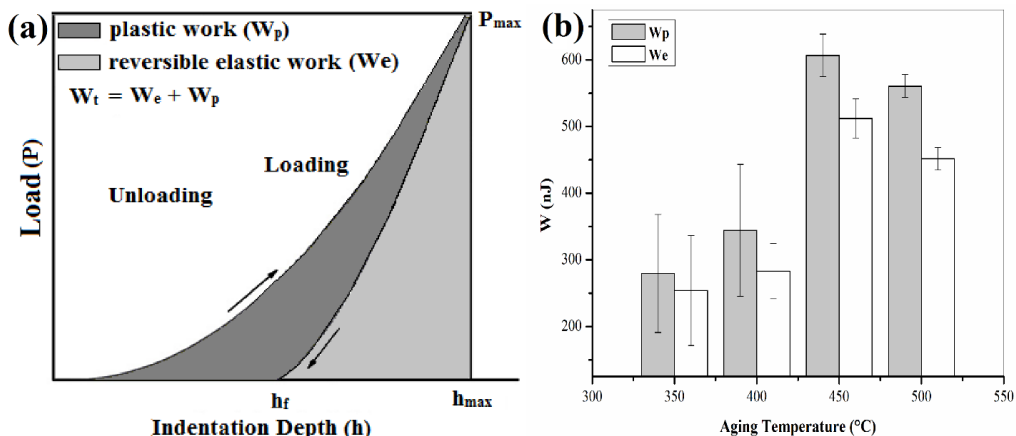


Fig. 8- (a) Comparison between W_p and W_e on load-indentation depth curve and (b) the extracted values of W_p and W_e from the load-indentation depth curves versus aging temperature.

References

1. Kumar A, Singh D, Kaur D. Variation in phase transformation paths of NiTi films as a function of film thickness. *Sensors and Actuators A: Physical*. 2012;178:57-63.
2. Chan PM, Chung CY, Ng KC. NiTi shape memory alloy thin film sensor micro-array for detection of infrared radiation. *Journal of Alloys and Compounds*. 2008;449(1-2):148-51.
3. Safavi MS, Azarniya A, Farshbaf Ahmadipour M, Reddy MV. New-emerging approach for fabrication of near net shape aluminum matrix composites/nanocomposites: Ultrasonic additive manufacturing. *Journal of Ultrafine Grained and Nanostructured Materials*. 2019 Dec 1;52(2):188-96.
4. Tillmann W, Momeni S. In-situ annealing of NiTi thin films at different temperatures. *Sensors and Actuators A: Physical*. 2015;221:9-14.
5. Hou H, Hamilton RF, Horn MW, Jin Y. NiTi thin films prepared by biased target ion beam deposition co-sputtering from elemental Ni and Ti targets. *Thin Solid Films*. 2014;570:1-6.
6. Tillmann W, Momeni S. Tribological performance of near equiatomic and Ti-rich NiTi shape memory alloy thin films. *Acta Materialia*. 2015;92:189-96.
7. Fernandes FMB, Martins R, Teresa Nogueira M, Silva RJC, Nunes P, Costa D, et al. Structural characterisation of NiTi thin film shape memory alloys. *Sensors and Actuators A: Physical*. 2002;99(1-2):55-8.
8. Morone A. Pulsed laser deposition of the NiTiCu thin film alloy. *Applied Surface Science*. 2007;253(19):8242-4.
9. Yang LM, Tieu AK, Dunne DP, Huang SW, Li HJ, Wexler D, et al. Cavitation erosion resistance of NiTi thin films produced by Filtered Arc Deposition. *Wear*. 2009;267(1-4):233-43.
10. Hasannaeimi V, Shahrebi T, Sanjabi S. Fabrication of NiTi layer via co-electrodeposition of nickel and titanium. *Surface and Coatings Technology*. 2012;210:10-4.
11. Jayachandran S, Mani Prabu SS, Manikandan M, Muralidharan M, Harivishanth M, Akash K, et al. Exploring the functional capabilities of NiTi shape memory alloy thin films deposited using electron beam evaporation technique. *Vacuum*. 2019;168:108826.
12. Sharma SK, Mohan S. Influence of annealing on structural, morphological, compositional and surface properties of magnetron sputtered nickel-titanium thin films. *Applied Surface Science*. 2013;282:492-8.
13. Satoh G, Birnbaum A, Yao YL. Annealing Effect on the Shape Memory Properties of Amorphous NiTi Thin Films. *Journal of Manufacturing Science and Engineering*. 2010;132(5).
14. Tillmann W, Momeni S. Comparison of NiTi thin films sputtered from separate elemental targets and Ti-rich alloy targets. *Journal of Materials Processing Technology*. 2015;220:184-90.
15. Pugina EV, Kornich GV. Temperature dependence of the sputtering yield of surface metal clusters. *Russian Physics Journal*. 2007;50(7):653-9.
16. Rumpf H, Winzek B, Zamponi C, Siegert W, Neuking K, Quandt E. Sputter deposition of NiTi to investigate the Ti loss rate as a function of composition from cast melted targets. *Materials Science and Engineering: A*. 2004;378(1-2):429-33.
17. Naveen Kumar Reddy B, Udayashankar NK. Influence of annealing temperature on the structural, morphological, mechanical and surface properties of near equiatomic NiTi thin films. *Vacuum*. 2017;142:186-96.
18. Miyazaki S, Fu YQ, Huang WM. *Thin Film Shape Memory Alloys: : fundamentals and device applications*. Cambridge University Press; 2009.
19. Tillmann W, Momeni S. Deposition of superelastic composite NiTi based films. *Vacuum*. 2014;104:41-6.
20. Tillmann W, Momeni S. Influence of in-situ and postannealing technique on tribological performance of NiTi SMA thin films. *Surface and Coatings Technology*. 2015;276:286-95.
21. Wang X, Van Humbeeck J, Verlinden B, Kustov S. Thermal cycling induced room temperature aging effect in Ni-rich NiTi shape memory alloy. *Scripta Materialia*. 2016;113:206-8.
22. Kustov S, Mas B, Salas D, Cesari E, Raufov S, Nikolaev V, et al. On the effect of room temperature ageing of Ni-rich Ni-Ti alloys. *Scripta Materialia*. 2015;103:10-3.
23. Kim JI, Miyazaki S. Effect of nano-scaled precipitates on shape memory behavior of Ti-50.9at.%Ni alloy. *Acta Materialia*. 2005;53(17):4545-54.
24. Khalil-Allafi J, Dlouhy A, Eggeler G. Ni₄Ti₃-precipitation during aging of NiTi shape memory alloys and its influence on martensitic phase transformations. *Acta Materialia*. 2002;50(17):4255-74.
25. Gong FF, Shen HM, Wang YN. Fabrication and characterization of sputtered Ni-rich NiTi thin films. *Materials Letters*. 1995;25(1-2):13-6.
26. Bechtold C, Chluba C, Zamponi C, Quandt E, de Miranda RL. Fabrication and Characterization of Freestanding NiTi Based Thin Film Materials for Shape Memory Micro-actuator Applications. *Shape Memory and Superelasticity*. 2019;5(4):327-35.
27. Khalili V, Khalil-Allafi J, Sengstock C, Motemani Y, Paulsen A, Frenzel J, et al. Characterization of mechanical properties of hydroxyapatite-silicon-multi walled carbon nano tubes composite coatings synthesized by EPD on NiTi alloys for biomedical application. *Journal of the Mechanical Behavior of Biomedical Materials*. 2016;59:337-52.
28. Mattox DM. *Handbook of Physical Vapor Deposition (PVD) Processing, Film Formation, Adhesion, Surface Preparation and Contamination Control*: Elsevier; 1998.
29. Khalil-Allafi J, Amin-Ahmadi B. Multiple-step martensitic transformations in the Ni₅₁Ti₄₉ single crystal. *Journal of Materials Science*. 2010;45(23):6440-5.
30. Khalil Allafi J, Ren X, Eggeler G. The mechanism of multistage martensitic transformations in aged Ni-rich NiTi shape memory alloys. *Acta Materialia*. 2002;50(4):793-803.
31. Khalil-Allafi J, Eggeler G, Dlouhy A, Schmahl WW, Somsen C. On the influence of heterogeneous precipitation on martensitic transformations in a Ni-rich NiTi shape memory alloy. *Materials Science and Engineering: A*. 2004;378(1-2):148-51.
32. Dlouhy A, Khalil-Allafi J, Eggeler G. Multiple-step martensitic transformations in Ni-rich NiTi alloys--an in-situ transmission electron microscopy investigation. *Philosophical Magazine*. 2003;83(3):339-63.
33. Kabla M, Seiner H, Musilova M, Landa M, Shilo D. The relationships between sputter deposition conditions, grain size, and phase transformation temperatures in NiTi thin films. *Acta Materialia*. 2014;70:79-91.
34. Oliver WC, Pharr GM. An improved technique for determining hardness and elastic modulus using load and displacement sensing indentation experiments. *Journal of Materials Research*. 1992;7(6):1564-83.
35. Behera A, Aich S, Behera A, Sahu A. Processing and Characterization of Magnetron Sputtered Ni/Ti Thin Film and their Annealing Behaviour to Induce Shape Memory Effect. *Materials Today: Proceedings*. 2015;2(4-5):1183-92.